Structural, electronic, and magnetic properties of nanometer-sized iron-oxide atomic clusters: Comparison between GGA and GGA+U approaches

Krisztián Palotás,* Antonis N. Andriotis, and Alexandros Lappas
Institute of Electronic Structure and Laser, Foundation for Research and Technology Hellas, P.O. Box 1385, Vassilika Vouton, 71110 Heraklion, Greece

(Received 4 June 2009; revised manuscript received 3 December 2009; published 2 February 2010)

We perform spin-polarized density-functional theory simulations within the generalized gradient approximation (GGA) and GGA+U method on nanometer-sized iron-oxide atomic clusters in different stoichiometries. By comparing total energies of structures with different symmetries and selected collinear magnetic configurations we find that low symmetry and, in general, ferrimagnetic structures exhibiting low total magnetic moment are energetically favorable. For the oxygen-rich $Fe_{25}O_{30}$ cluster we obtain a cagelike geometry with a few ions within the cage that seem to stabilize the structure. Considering the $Fe_{33}O_{32}$ cluster of nanometer-size we propose the formation of a rocksalt type structure, which is characteristic of bulk FeO. Based on data of iron *d* shell electron occupancies, we exclude double exchange from possible magnetic interactions between iron ions, and we point to a competition between direct exchange and superexchange, where the dominant interaction is determined by the cluster topology. For the smaller $Fe_{13}O_8$ cluster we find ferromagnetic energetically favorable geometries of lower symmetry than previously reported. Our results demonstrate the importance of going beyond GGA, in particular, physical properties obtained within GGA+U description are found to be remarkably different from those using GGA. In order to confirm our theoretical predictions, cluster experiments in this size regime are desirable.

DOI: 10.1103/PhysRevB.81.075403 PACS number(s): 61.46.−w, 73.22.−f, 75.75.−c

I. INTRODUCTION

Magnetic nanomaterials can be promising in use as building blocks for future technological applications. Understanding their physical and chemical properties is, therefore, essential for fabricating complex nanodevices in a controlled way, even at the industrial level, e.g., in the fields of magnetic data storage[1,2] or biomedicine.[3] Device lifetime is a relevant issue which has to be taken into account in the design process and which can be modified by the chemical environment. Under normal conditions oxidation is a naturally occurring process. It is well known that oxidation of ferromagnetic materials is likely to be able to destroy the highly desired (ferro)magnetic properties and change it to ferrimagnetism or antiferromagnetism,[4] which is less favorable particularly for magnetic data storage purposes. The understanding of oxidation in transition metal (TM) oxides at the nanoscale is also theoretically challenging since size and shape effects can drastically modify the structure itself and, thus, magnetic order in finite structures.[5] In such systems strong surface anisotropy can be observed and modeled.[6,7] Another theoretical interest is concerned with the evolution of physical properties, for example electric transport properties,[8] as materials grow from the atomic to the macroscopic scale.

Considering these practical and theoretical issues we perform density functional theory (DFT) simulations on nanometer-sized iron-oxide atomic clusters in different stoichiometries. We focus on the comparison of physical properties using GGA and GGA+U electron density approximations. DFT+U methods have already been extensively used for describing electronic structure of strongly correlated bulk materials of TM oxides,[9] particularly iron oxides.[10–16] Catalytic properties have been studied not only on TM-oxide surfaces using the GGA+U approach,[17] but also on small iron-oxide clusters within GGA.[18–21] Other possibilities for theoretical description of strongly correlated electron systems include the so-called self-interaction correction (SIC) method (Ref. 22 and references therein) and DFT using hybrid functionals (Ref. 23 and references therein). In our study, however, we use the GGA+U approach for investigating iron-oxide clusters. The impact of going beyond GGA in TM-oxide atomic clusters is discussed intensively, particularly comparing our findings with those found in the literature. To the best of our knowledge there are hardly any studies employing GGA+U. During the completion of the present investigation we became aware of the work of López *et al.*[24] on which we comment in the next sections. Our results demonstrate that considerable structural changes of the clusters occur when switching from GGA to GGA+U, which may result in a concomitant change in magnetic properties.

First, we review several experimental and theoretical results on iron-oxide clusters: Wang *et al.*[25] studied sequential oxygen atom chemisorption on small Fe clusters (Fe_nO_m, $n=1-4$, and $m=1-6$) and measured photoelectron spectra of the anionic compounds, thus, the electronic excitation spectra of neutral clusters. They found that the electron affinity increases with increasing degree of oxidation and the dependence is linear for Fe_3O_n and Fe_4O_n. They also speculated on the possible geometric arrangement of the atoms in the clusters and suggested a bridge site adsorption of oxygen based on previous results.[26] Griffin *et al.* performed experimental research on reactions of iron clusters with O_2 and determined bond energies for Fe_nO^+ and $Fe_nO_2^+$ ($n=2-18$).[27]

Research on "magic" clusters intensified at the second half of the 1990s. Small iron-oxide clusters have been produced by using, e.g., a reactive laser vaporized cluster source. Analyzing mass spectra of the produced clusters re-

vealed "magic numbers," i.e., some specific compounds were preferred compared to others suggesting that they are also more stable. *Ab initio* calculations have been used to investigate their structural, electronic, and magnetic properties which turned out to be quite successful. A well-studied example is the $Fe_{13}O_8$ cluster.[28,29] It has first been produced by Wang *et al.*[28] *Ab initio* calculations reveal that the ground-state geometry has a D_{4h} symmetry with a core of Fe_{13} on which eight oxygen atoms are adsorbed. Its binding energy as well as its highest occupied molecular orbital (HOMO)-lowest unoccupied molecular orbital (LUMO) gap is much larger than closely related clusters thus confirming the experimental results of its stability. $Fe_{13}O_8$ has also been found intrinsically stable[30] from calculations of its vibrational properties. Another theoretical research focused on the detailed study of the magnetic structure of $Fe_{13}O_8$ and proved that a ferromagnetic state having a total magnetic moment of $32\mu_B$ is the most stable.[31] Moreover, magnetic anisotropy energy of 33.4 K has been calculated for the above system. High magnetic moment and relatively high anisotropy energy could make this particular cluster a promising candidate for nanomagnetic applications. Kortus *et al.*[31] have also calculated vibrational properties and corrected the results of Sun *et al.*[30] Later, gold coating of the model system $Fe_{13}O_8$ has been considered in order to model biocompatible clusters and the extent of bioseparation of amino acids has been investigated,[32] which is useful for possible biomedical applications, particularly for targeted drug delivery.

Another magic cluster has been suggested by mass spectroscopy data in the work of Sun *et al.*:[33] They produced M_9O_6 clusters with M=Fe, Co, and Ni and using *ab initio* calculation they concluded that the most stable geometry shows C_{2v} symmetry. Analyzing the calculated electronic structures [density of states (DOS)] they found that the majority $3d$ level of Ni hybridizes stronger with the O $2p$ states thus O atoms are ferromagnetically (FM) polarized while for Fe and Co the minority $3d$ levels have stronger hybridization with O $2p$ and an antiferromagnetic (AFM) polarization for O atoms occurs. The above mentioned magic clusters have been produced experimentally under oxygen deficient conditions. However, it is possible to create clusters of close to one to one stoichiometry in the presence of appropriate amount of oxygen during the production process. Shin *et al.*[34,35] found that the most stable clusters are of the form of Fe_nO_n, Fe_nO_{n+1}, and Fe_nO_{n+2}. More oxygen-rich structures dominate above n=10. They also found that $Fe_nO_{n-1,2}$ can also be observed although they are less abundant than others. In order to contribute to the theoretical understanding of iron-oxide formation, Shiroishi *et al.*[36] studied small Fe_nO_m clusters and found that the structures suggested by Wang *et al.*[25] are basically correct and AFM Fe moment alignment develops with increasing number of oxygen atoms at $m=n$ for n=2, 3, and 4. They also found a noncollinear magnetic configuration, with a total magnetic moment of zero, as the ground state for the Fe_3O_5 cluster.

Kirilyuk *et al.*[37] suggested a geometry for Co_4O_4 similar to bulk CoO (rock salt) and studied the different (FM and AFM) moment alignments on the structure. The ground state is found to be FM and undistorted, whereas the AFM alignment brought a significant distortion to the geometry, which is not energetically favorable. In contrary, Jones *et al.*[38,39] showed theoretical evidence within GGA that stable rings are the preferred structures for Fe_nO_n of up to n=5. Above this size, nanotowers and cages develop by increasing the number of atoms in the cluster and keeping the stoichiometry constant. It has also been shown that hollow drums can also form by slightly going to the O-rich regime, i.e., for Fe_nO_{n+1} and Fe_nO_{n+2}, which, in fact, stabilizes the structure. The towers are formed by attaching individual rings together, for which, it has been shown that the interring interactions are weaker than intraring interactions. For example, Fe_9O_9 is formed by attaching three Fe_3O_3 rings together. This development of iron oxide, from small cluster sizes toward the bulk, has recently been questioned by Molek *et al.*[40] who studied photodissociation of iron-oxide cluster cations. Taking as example the Fe_9O_9 cluster (denoted by 9/9) they did not find much intense fragments of Fe_6O_6 (6/6) which should be formed first by breaking the (weaker) interring bonds between Fe_6O_6 (6/6) and Fe_3O_3 (3/3), as suggested by Jones *et al.*[38] Instead, they found more intense fragments of 2/2, 3/3, 4/4, and 5/5, with 3/3 being the most intense one. This could be, however, explained by simultaneous interring bond breakings providing three Fe_3O_3 rings out of one Fe_9O_9 cluster.

In a recent paper, Ding *et al.* studied $(Fe_2O_3)_n$ cage and noncage clusters using DFT with a B3LYP hybrid functional.[23] They found that although the cage structures are stable up to a certain size, most of the considered noncage clusters with lower (mostly C_1) symmetry are energetically favorable compared to the cages. For a different TM-oxide cluster, Co_nO_n (n=4,6,9,12), the same group showed that tower or cage structures are energetically more stable than rocksalt type clusters.[41]

Since the formation of bulk iron oxides following a bottom-up approach is still not completely understood the present study tries to add to the understanding of this phenomenon in two ways: first, in contrast to most of the earlier reports, we use an improved method for describing the electronic states of the strongly correlated iron-oxide clusters, namely, DFT+U. Second, we investigate atomic clusters having a diameter of about one nanometer ($Fe_{25}O_{30}$ and $Fe_{33}O_{32}$, containing 55 and 65 atoms, respectively), considerably larger than previously studied by *ab initio* calculations with the exception of the recent paper by López *et al.*[24] whose research focus was different than ours. While their cluster geometries were motivated by two different phases of bulk magnetite and they compared physical properties between clusters and bulk, we are focusing on four issues: first, we compare total energies of cluster structures having high symmetry (T_h and O_h) with those obtained by symmetry-unrestricted calculations (C_1 symmetry). Second, we compare energetics of ferromagnetic and ferrimagnetic configurations. We find that low symmetry and, in general, ferrimagnetic structures are energetically favored. Third, we suggest that the magnetic interactions between iron ions depend on the topology of the cluster and for a specific stoichiometry range double exchange can be excluded due to electronic structure. Additionally, we point to a competition of direct exchange and superexchange in determining this interaction. Fourth, we study the structural, electronic and mag-

netic properties depending on the description of the electron density, namely, comparing GGA and GGA+U methods, where we find remarkable differences. Furthermore, we show results for the $Fe_{13}O_8$ cluster, where energetically favorable structures of low symmetry (C_1) are obtained, in contrast to the previously reported structures with D_{4h} symmetry.[28,30,31]

II. COMPUTATIONAL DETAILS

We perform calculations based on DFT at the spin-polarized generalized electron density gradient approximation (SGGA), as well as at the SGGA+U level of approximation as implemented in the Vienna *ab initio* simulation package (VASP).[42–45] Here, the notations SGGA and SGGA+U have been introduced before,[17] where U refers to a Hubbard term describing the on-site Coulomb electron-electron repulsion. We use the simplified rotationally invariant DFT+U model developed by Dudarev *et al.*,[46] in which an effective $U^\star = U - J$ incorporates the on-site Coulomb (U) and the exchange (J) interactions. A plane-wave basis set for electronic wave function expansion together with the projector augmented wave (PAW) method[47] has been used while the exchange-correlation functional is parametrized according to Perdew and Wang (PW91).[48] The cut-off energy was consistently set to 400 eV in all calculations. Cluster geometries have been optimized by applying a conjugate gradient algorithm. Since one of the main focuses of this study is a comparison between high and low symmetry structures in the nanometer-size range some structural optimizations have been performed with symmetry constraints while others without. The convergence criteria for total energy and force were 10^{-4} eV and 10^{-2} eV/Å, respectively. In all calculations, the clusters are placed in a cubic cell with edge length of 20.37 Å with periodic boundary conditions which provides an adequate surrounding vacuum region around the cluster (10–16 Å depending on the cluster type) to make dispersion effects negligible. The large supercell makes it possible to use just one k point (Γ) representing the Brillouin zone. For analyzing the bond characteristics the maximum (cut-off) bond lengths of 2.4 and 2.9 Å have been chosen for the Fe-O and Fe-Fe bonds, respectively. Interatomic distances above these values are not considered as bonds and are not counted in the bond statistics.

For electron DOS calculations a Gaussian smearing factor of 0.01 has been taken. Moreover, we deal with collinear magnetic configurations only and the reported magnetic moments refer to pure spin moments without any orbital moment contributions throughout the paper. Thus, spin-orbit coupling is also neglected. The spin moments have been calculated by integrating the spin density within the atomic radii of 1.302 and 0.820 Å for Fe and O, respectively. Ionic charges have been obtained by using grid-based Bader charge analysis as implemented by Henkelman and co-workers.[49–51] We used a $168 \times 168 \times 168$ fine grid for storing the charge density which corresponds to a distance of 0.12 Å between nearest neighbor grid points.

The value of U in the SGGA+U approach is usually obtained by fitting simulated physical properties to experimentally observed ones (e.g., photoelectron absorption peak positions for atomic clusters or band gap for bulk materials).[16] Here, the U value for the best match of the considered physical characteristics provides a parameter to be used for future simulations. In the present work we use U values obtained from previous bulk calculations for two reasons: (i) first, we did not find available experimental data in the literature on photoelectron spectra for the studied size range of the clusters, thus, we cannot make any comparisons as described above. Photoelectron spectrum for the maximal size of Fe_4O_6 has been measured by Wang *et al.*[25] Production of clusters via the laser vaporization technique is also limited by experimental conditions and detection capabilities. Analysis of the time-of-flight mass spectra shows that the clearly obtainable peak corresponds to a stable iron-oxide cluster having a maximum size of about 48 atoms (composition $Fe_{23}O_{25}$, see Fig. 3 in Ref. 34). (ii) Second, present study focuses on the comparison of structural, electronic and magnetic properties of iron-oxide clusters by comparing the SGGA and SGGA+U approaches used in the calculations, i.e., we contrast results obtained by using zero and a single positive U value chosen from a range found in the literature and we do not apply the self-consistent Hubbard U approach proposed earlier.[52,53] Reported theoretical works on different bulk iron oxides have considered the $U^\star$ value in the range of 3.5–6.0 eV.[9–16] Guided by these reports we choose the value of $U^\star = 5$ eV for the Fe d states in the SGGA+U approach, while SGGA corresponds to the zero value of $U^\star$.

III. RESULTS AND DISCUSSION

In this part, calculated physical properties for the clusters $Fe_{13}O_8$, $Fe_{25}O_{30}$, and $Fe_{33}O_{32}$ are presented and discussed. From these the latter two are in the nanometer-size range, while $Fe_{13}O_8$ has been chosen because of comparison reason since there are theoretical and experimental studies reporting on this system. Note that the considered clusters correspond to different stoichiometric compositions of iron oxide ranging from close to one to one stoichiometry ($Fe_{33}O_{32}$) to oxygen rich ($Fe_{25}O_{30}$) and oxygen deficient clusters ($Fe_{13}O_8$).

A. $Fe_{13}O_8$

We calculated $Fe_{13}O_8$ clusters from many starting geometries using SGGA and SGGA+U ($U^\star = 5$ eV). Symmetry constraint has been applied to the considered relaxed high symmetry (O_h and D_{4h}) clusters, while symmetry-unrestricted relaxations always led to low symmetry (C_1) geometries, in contrast to earlier works.[28,31,32] Here, we report details on the obtained energetically most favorable geometries and their corresponding ferromagnetic structures. The dependence of the HOMO-LUMO gap on the Hubbard U parameter for two different relaxed geometries is also presented.

Relaxed structures are shown in Fig. 1. The results for bond lengths, ionic charges, magnetic moments, and relative total energies are summarized in Table I. Here, in the top panel the number of bonds for each type is explicitly shown in parenthesis. In O_h symmetry there are two nonequivalent

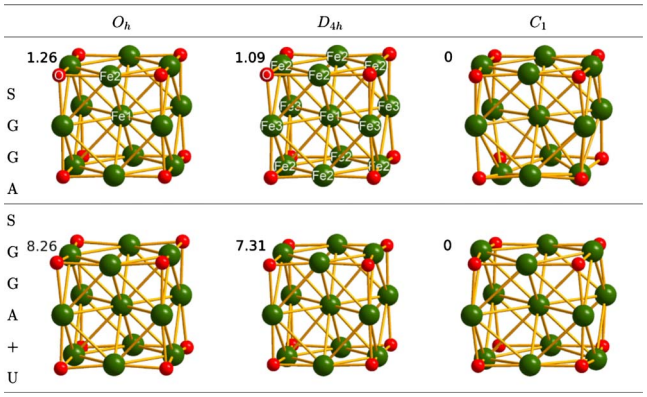

FIG. 1. (Color online) Relaxed geometries of the $Fe_{13}O_8$ cluster obtained from the O_h restricted (left), D_{4h} restricted (middle), and symmetry-unrestricted (C_1) (right) optimizations using the SGGA (top line) and SGGA+U ($U^{\star}=5$ eV) (bottom line) approaches. Each structure is labeled (at the top left part) by its total energy (in eV) relative to the calculated lowest value, which is denoted by zero. Note that comparison of energies is only meaningful within particular lines using the same approximation. Fe and O atoms are denoted by green (dark) and red (light) colors, respectively. Bonding and magnetic properties of these structures are reported in Table I.

Fe atoms, i.e., central and surface iron labeled by Fe1 and Fe2, respectively, while in D_{4h} symmetry there are two different surface Fe atoms. In this latter case we adopted the notations of Wang *et al.*[28] for better comparison, i.e., Fe1 refers to the central atom and we have eight Fe2 and four Fe3 surface sites. In both O_h and D_{4h} cases the O atoms are equivalent by symmetry reasons.

Comparing bond lengths for the D_{4h} symmetry structure obtained within SGGA to earlier studies[28,31,32] we find good agreement. Analyzing the changes of the bond lengths when switching from SGGA to SGGA+U description we point out the following: In the cluster of O_h symmetry the Fe-Fe bond lengths slightly decrease, while the lengths of Fe-O bonds increase by turning on the on-site Coulomb interaction (U) for the iron species. Concomitantly, we find that the mean of the ionic charges does not change significantly for this high-symmetry cluster, however, the central Fe1 atom becomes negatively charged, which explains the Fe-Fe bond decrease. On the other hand, we find systematic bond increase of all types in the other clusters when turning on U. The Fe-Fe bond increase can be explained by the enlarged ionic charges on the species which cause electrostatic repulsion between iron cations. However, the increase in Fe-O bond lengths cannot be explained in this simple way due to their mixed ionic-covalent nature.[23] In fact, less electron localization is indicated on the O species by the following: integrating the electron density within the atomic radius of 0.820 Å results in approximately five electrons around the oxygen atoms, whereas Bader charge analysis assigns on average about 7–7.2 electrons to an oxygen. On the other hand, electrons on iron atoms seem to be more localized since there is a minor difference in the number of electrons on iron atoms calculated either by integration or Bader analysis. Checking the orbital occupancies of the electrons reveals that there is a significant charge transfer from the Fe *s* electrons toward the Fe-O bond, while the occupancy of the Fe *d* shell is close to the neutral iron atom (not shown for $Fe_{13}O_8$, but see bottom parts of Fig. 6 and Fig. 8 for bigger clusters). Furthermore, we gain information about the Fe-O hybridization by plotting the projected electron density of states (PDOS) for nearest-neighbor iron and oxygen atoms. Fe *d*-type and O *p*-type PDOS are shown if Fig. 2 for the C_1 symmetry cluster obtained at SGGA and SGGA+U. The results suggest less hybridization, particularly near the Fermi energy, and, consequently, weaker bonds between iron and oxygen in the relaxed clusters calculated by using SGGA+U, which explains the increased Fe-O bond lengths.

Elongated bonds have also been reported for Fe_2 and FeO^+ within the self-consistent GGA+U approach by Kulik *et al.*[53] and evidence for structural changes depending on ionic charges has been studied in MgO clusters by Johnston.[54] Comparing ionic charges in our D_{4h} symmetry cluster using SGGA to those reported by Wang *et al.*,[28] we find significant differences, which can possibly be attributed to the different methods used for charge evaluation; we used Bader charge analysis.[49–51] The most striking difference is their negatively charged central atom, which turns out to be energetically unfavored in our other cluster (O_h, SGGA+U). Altogether, we believe that the remarkably high percentual increase in the mean Fe-Fe bond length (10%) in the C_1 symmetry cluster upon turning on the on-site electron-electron interaction (U) might point to a reconsideration of previously reported GGA-based TM and TM-oxide cluster structures. Comparison to experimentally observed geometries would help a lot to clarify whether GGA or GGA+U is better suited for describing iron oxide, and more generally TM-oxide clusters.

Comparing our results for the D_{4h} symmetry cluster within SGGA to earlier studies[28,31,32] we find good agreement for the total spin moment, average iron moment and the relative (opposite) direction of O moments with respect to Fe. We also find that the central Fe1 atom has the largest moment. However, in our case the magnitude of surface Fe3 moment is larger than that of the Fe2 site, which is due to different coordination geometry. This is a very illustrative example of how slightly different cluster structures may result in different magnetic states. This situation changes even more when studying cluster properties within SGGA+U. Applying $U^{\star}=5$ eV the average Fe moment is enhanced, particularly due to the increased moments on surface sites and the relative order of Fe moments changes to $\mu_{Fe3} > \mu_{Fe2} > \mu_{Fe1}$. The O moment alignment turns to be parallel relative to Fe instead of being antiparallel at SGGA. On the other hand, the spin polarization of the O atoms remains very small in D_{4h} symmetry clusters, resulting in small induced magnetic moments.

In the cluster of O_h symmetry the spin moments on the surface Fe2 atoms are consistently larger than on the central Fe1 for both employing SGGA and SGGA+U. This is understandable since surface iron atoms have a smaller coordination number (five Fe and two O neighbors) than the central one (12 Fe neighbors). Again, the average Fe moment is enhanced by applying the Hubbard U term. However, for this symmetry the O moment alignment changes from being par-

TABLE I. Physical properties of the relaxed $Fe_{13}O_8$ clusters in three symmetries, the O_h restricted, D_{4h} restricted, and the unrestricted one (C_1), obtained by using the SGGA ($U^\star=0$) and SGGA+U ($U^\star=5$ eV) approaches. Exact and average bond lengths, ionic charges, atomic, average, and total magnetic moments and total energies relative to the lowest energy structure found for using the corresponding method are shown. Numbers in parentheses refer to the number of bonds of the corresponding type in the bond lengths panel and to the number of that particular atom (see text for details) in the other two panels. Reported values in this table belong to structures shown in Fig. 1.

$Fe_{13}O_8$	Symmetry O_h			Symmetry D_{4h}			Symmetry C_1		
				Bond lengths (Å)					
Method	SGGA		SGGA+U	SGGA		SGGA+U	SGGA		SGGA+U
$r_{Fe1\text{-}Fe2}$	2.595	(12)	2.559	2.466	(8)	2.654			
$r_{Fe1\text{-}Fe3}$				2.491	(4)	2.656			
$r_{Fe2\text{-}Fe2}$	2.595	(24)	2.559	2.380	(8)	2.482			
$r_{Fe2\text{-}Fe3}$				2.521	(16)	2.740			
$\langle r_{Fe\text{-}Fe}\rangle$	2.595	(36)	2.559	2.474	(36)	2.654	2.552	(36)	2.804
$r_{Fe2\text{-}O}$	1.877	(24)	1.932	1.852	(16)	1.916			
$r_{Fe3\text{-}O}$				1.855	(8)	1.925			
$\langle r_{Fe\text{-}O}\rangle$	1.877	(24)	1.932	1.853	(24)	1.919	1.888	(24)	1.909
				Ionic charges [$\lvert e\rvert$]					
Method	SGGA		SGGA+U	SGGA		SGGA+U	SGGA		SGGA+U
q_{Fe1}	+0.184	(1)	−0.149	+0.048	(1)	+0.125			
q_{Fe2}	+0.752	(12)	+0.783	+0.688	(8)	+0.831			
q_{Fe3}				+0.675	(4)	+0.725			
$\langle q_{Fe}\rangle$	+0.708	(13)	+0.711	+0.635	(13)	+0.744	+0.630		+0.701
$\langle q_O\rangle$	−1.151	(8)	−1.155	−1.031	(8)	−1.209	−1.024		−1.139
				Magnetic moments [μ_B]					
Method	SGGA		SGGA+U	SGGA		SGGA+U	SGGA		SGGA+U
μ_{Fe1}	2.848	(1)	2.719	2.788	(1)	2.896			
μ_{Fe2}	3.014	(12)	3.317	2.148	(8)	3.223			
μ_{Fe3}				2.660	(4)	3.232			
$\langle \mu_{Fe}\rangle$	3.001	(13)	3.271	2.355	(13)	3.201	2.882		3.359
$\langle \mu_O\rangle$	0.143	(8)	−0.062	−0.002	(8)	0.005	0.122		0.040
Total moment	40.2		42.0	30.6		41.6	38.4		44.0
Rel. total energy (eV)	1.26		8.26	1.09		7.31	0.00		0.00

allel to antiparallel relative to Fe moments. Concomitantly, the magnitude of the induced moment drops but it is still much higher than for the D_{4h} case. This is also true for the cluster with C_1 symmetry but here O moments are consistently parallelly aligned relative to Fe for both applying SGGA and SGGA+U. Altogether, in this oxygen deficient cluster most likely the direct exchange mechanism governs the FM iron moment alignment as iron atoms form a compact region and are directly coupled.

Turning to the question of energetic stability we analyze the total energies of the reported clusters. Relative values with respect to the lowest total energy are found in the last row of Table I. It has to be noted that meaningful comparison can only be made between calculated total energies using the same $U^\star$ value, therefore, in our case we have two reference zero values for $U^\star=0$ and 5 eV, respectively. These correspond to the energetically most stable clusters. It can clearly be seen that clusters with C_1 symmetry are the most stable for both employing SGGA and SGGA+U approaches. This finding opposes results of previous theoretical studies,[28,30–32] where clusters of D_{4h} symmetry have been reported as the ground state for the $Fe_{13}O_8$ system. In our case the most stable D_{4h} symmetry cluster is 1.09 eV higher in energy than that of C_1 symmetry within SGGA. This energy difference increases to a much higher value of 7.31 eV when using SGGA+U. Relaxed structures with O_h symmetry have even higher total energies compared to D_{4h}, thus, these geometries can be excluded from possible ground states. Summarized, from energetic analysis, we propose C_1 symmetry ground-state cluster geometries, which should possibly be verified by experiments.

One of the reasons to find different structures compared to the previously reported ones might be that Kortus *et al.*[31] used a different Gaussian-orbital-based method, while Wang *et al.*[28] employed the same VASP code as we do but with ultrasoft pseudopotentials for describing electron-ion interactions. Instead, we applied the PAW method.[47] Moreover, different convergence criteria for the forces acting on the individual atomic sites during geometry optimization have been applied: 0.03[28] and 0.05 eV/Å,[31] whereas we had a more strict criterium of 0.01 eV/Å. Another difference between present and previous calculations is the size of the supercell

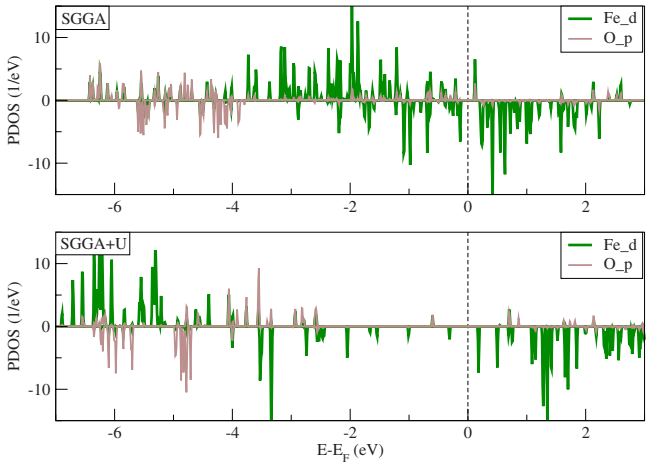

FIG. 2. (Color online) Electron PDOS of nearest neighbor Fe and O atoms in the C_1 symmetry clusters of $Fe_{13}O_8$ stoichiometry obtained within SGGA (top part) and SGGA+U (bottom part). Fe d-type and O p-type PDOS are shown in order to highlight the Fe-d–O-p hybridization.

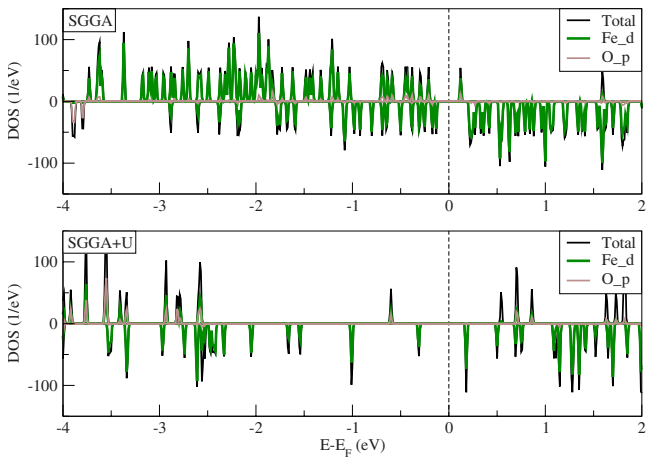

FIG. 3. (Color online) Total electron DOS of the energetically preferred C_1 symmetry clusters of $Fe_{13}O_8$ stoichiometry obtained within SGGA (top part) and SGGA+U (bottom part). Contributions from Fe d-type and O p-type states are highlighted in green (medium) and gray (light) colors, respectively. Corresponding geometries are shown in the rightmost column of Fig. 1.

where the clusters are placed. We used a considerably larger supercell, thus, reduced the interactions between clusters in neighboring cells.

In order to get more insight to the clusters, we studied their electronic structure by calculating electron DOS. Total DOS and contributions from Fe d and O p states are shown in Fig. 3 for the C_1 symmetry cluster obtained at SGGA and SGGA+U. The insulating character of the clusters can clearly be seen for both descriptions indicated by an energy gap at the Fermi level. Apart from that, we see that electron DOS comes mostly from d states of irons for SGGA, while p states of oxygens appear to have more importance for majority spin electrons at SGGA+U. Moreover, following the definitions of Kortus *et al.*[31] we calculated the spin gaps for the relaxed C_1 and D_{4h} symmetry structures and we found all of them positive. It means that the obtained magnetic states for these structures are at least metastable.[31] The HOMO-LUMO gap we consider corresponds to the minimum of the four possible energy gaps between majority ($\uparrow$) and minority ($\downarrow$) HOMO and LUMO energy levels, i.e.,

$$E_{gap} = \min(-E^{\alpha}_{HOMO} + E^{\beta}_{LUMO});$$

$$(\alpha,\beta) = (\uparrow,\uparrow),(\downarrow,\downarrow),(\uparrow,\downarrow),(\downarrow,\uparrow). \quad (1)$$

We obtain a HOMO-LUMO gap of 0.25 eV for C_1 and 0.06 eV for D_{4h} symmetry cluster within SGGA. The former value is much higher than previously reported for D_{4h} symmetry clusters,[28,31] which suggests that the lower-symmetry cluster is indeed more stable than that of D_{4h} symmetry. The electronic stability is further increased employing SGGA+U, where we obtain a HOMO-LUMO gap of 0.49 eV for the relaxed cluster with C_1 symmetry, which is still larger than 0.34 eV for D_{4h} symmetry.

Finally, we investigate the U-dependent electronic structures for the most stable C_1 symmetry geometries. This study provides insight into the relationship between the extent of electron localization (parametrized by U*) and electronic and magnetic properties of a prototypical low dimensional iron-oxide cluster. Keeping the structure fixed we study the dependence of the HOMO-LUMO gap as well as average iron magnetic moments on the U* parameter in the interval between 0 and 5 eV. We report two sets of the above data for the two different relaxed structures, one obtained by the SGGA and the other by the SGGA+U approach used during geometry optimization. We find that the HOMO-LUMO gap corresponds almost exclusively to the energy difference between minority spin $E^{\downarrow}_{HOMO}$ and $E^{\downarrow}_{LUMO}$ levels for both structures and applied U* values. The only exception is the SGGA structure and U*=0 eV, where the minimum in Eq. (1) is found for the spin gap of $(-E^{\downarrow}_{HOMO}+E^{\uparrow}_{LUMO})$, see also top part of Fig. 3. The U* dependence of the HOMO-LUMO gaps and the average iron moments is shown in Fig. 4. It can be seen that for both geometries the energy gaps tend to increase as going to higher values of U*. This increase is monotonous for the SGGA+U structure while nonmonotonous for the SGGA one. This behavior is also true for the iron moments: they increase monotonously with growing U* in both geometries. For the SGGA+U structure the gap increase is almost linear up to U*=3 eV, which is followed by a jump as switching to U*=4 eV and again linear with the previously observed slope as reaching U*=5 eV. The magnetic moments of iron in this geometry follow the same trend but here the linear dependence is more obvious in the U* $\leq$3 eV regime. For the SGGA structure the gap evolution is not that simple, it shows an oscillating behavior but also a growing tendency. On the other hand, the average iron moment jumps when going from U*=0 to 1 eV and then it shows a linear growth with increasing U*. Similarly, increase of the band gap and magnetic moments with increasing U has been reported for iron-oxide bulk materials,[10–16] although these dependencies have not been analyzed in detail. It is interesting to note that Wang *et al.*[9] report linear dependence of oxidation energies in various TM oxides. We found two different evolution characteristics for the U* dependence of

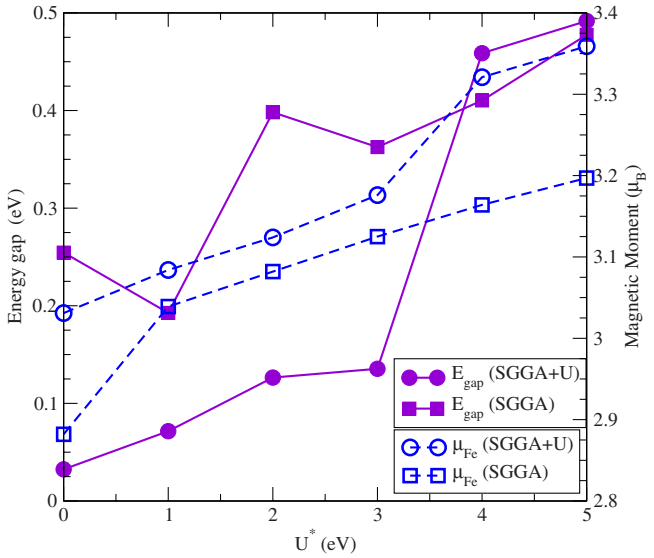

FIG. 4. (Color online) HOMO-LUMO gaps (E_{gap}) and average Fe magnetic moments (μ_{Fe}) plotted versus the Hubbard U* parameter for two relaxed structures of C_1 symmetry $Fe_{13}O_8$ obtained at the SGGA and SGGA+U levels of approximation. Geometries are shown in the rightmost column of Fig. 1.

HOMO-LUMO gaps in our clusters, one is linear with a certain jump and another with an oscillatory behavior that need further studies for better understanding.

B. $Fe_{25}O_{30}$

Next, we consider clusters in the nanometer-size range and we are interested whether high- or low-symmetry structures are energetically favorable. The results of Ding *et al.*[23] suggest that structures of lower symmetry can be energetically preferred for a specific oxygen-rich iron-oxide stoichiometry in a similar size range. López *et al.*[24] also found that a lower symmetry monoclinic phase of iron-oxide clusters is energetically more stable than a cubic phase. Going beyond all that we report another insight to the clusters by studying their magnetic properties, i.e., we compare energetics of ferromagnetic and ferrimagnetic configurations for both SGGA and SGGA+U descriptions. As discussed in the previous section, there are remarkable differences between calculated physical properties of clusters depending on the U* parameter. Its proper value should be chosen based on a combination of simulations and results from advanced cluster experiments. However, to the best of our knowledge, there are no low-temperature experimental investigations to date, where information about the cluster structure in this size regime can be extracted. This may be due to the experienced lower signal to noise ratio for time-of-flight mass spectrometry with increasing cluster size.[35]

Choosing the oxygen-rich composition $Fe_{25}O_{30}$ we build an initial cluster structure of T_h symmetry. Keeping this symmetry we perform structural optimizations with FM iron moment alignment as constraint. The relaxed cluster geometries are shown in the left column of Fig. 5 obtained within SGGA and SGGA+U, respectively. Due to symmetry there

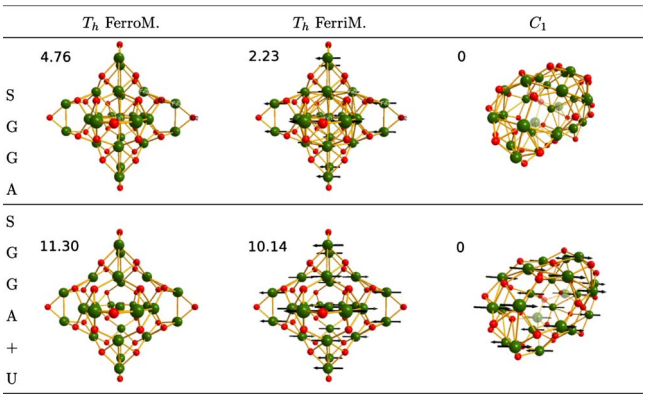

FIG. 5. (Color online) Relaxed geometries of the $Fe_{25}O_{30}$ cluster obtained from the T_h-restricted (left and middle) and symmetry-unrestricted (right) optimizations using the SGGA (top line) and SGGA+U (U*=5 eV) (bottom line) approaches. Each structure is labeled (at the top left part) by its total energy (in eV) relative to the calculated lowest value, which is denoted by zero. Note that comparison of energies is only meaningful within particular lines using the same approximation. Geometries in the left and middle column correspond to ferromagnetic and ferrimagnetic configurations, respectively. For the C_1 symmetry cluster the structures of the energetically preferred ferromagnetic and ferrimagnetic states are shown in the right column for SGGA (top part) and SGGA+U (bottom part), respectively. Fe atomic magnetic moment vectors for the ferrimagnetic configurations are explicitly shown. Fe and O atoms are denoted by green (dark) and red (light) colors, respectively. Bonding and magnetic properties of these structures are reported in Table II.

are three nonequivalent Fe atoms: one central Fe1, twelve surface irons (Fe2), which are directly bound to Fe1 and twelve other surface irons (Fe3), which have no direct bonds to the central iron atom. Furthermore, we have two nonequivalent oxygen atoms: twenty-four O1 are bound to both Fe2 and Fe3 type of atoms, whereas six O2 are connected to Fe3 atoms only. Taking these relaxed geometries we calculate four collinear magnetic configurations by keeping the direction of the central iron (Fe1) moment fixed: [Fe1,Fe2,Fe3]=[↑↑↑],[↑↑↓],[↑↓↑],[↑↓↓]. Comparing their total energies we find that such a magnetic configuration is preferred where Fe1 and Fe2 moments point to the same direction, whereas Fe3 moments are of opposite direction, i.e., [Fe1,Fe2,Fe3]=[↑↑↓]. Relaxing the geometry of this ferrimagnetic cluster we arrive at the structure shown in the middle column of Fig. 5. Here, the atomic magnetic moments are indicated by vectors. Starting from different initial systems by turning off the symmetry constraint in the geometry optimization we obtain relaxed structures with C_1 symmetry. For these systems we consider FM and one specific ferrimagnetic iron moment alignment. In the SGGA case we find a FM cluster energetically preferred, although, its ferrimagnetic state is only 0.09 eV higher in total energy. In contrast, by using SGGA+U a ferrimagnetic cluster is preferred, which beats the FM state by 0.36 eV. The obtained structures with the lowest total energy are shown in the right column of Fig. 5. Note that the possibility cannot be excluded that by considering a different arrangement of magnetic moments another ferrimagnetic state would be energeti-

cally preferred, however, a systematic calculation of all magnetic states would be quite demanding and we did not focus on this issue.

Interestingly, the energetically preferred C_1 symmetry clusters are like cages and do not have compact geometries. For both SGGA and SGGA+U cases, by removing one oxygen and two iron atoms from the middle we arrive at a proper cage. The cage consists of 22 Fe_2O_2 and 14 Fe_3O_3 rings[38] in the SGGA case, while 26 Fe_2O_2 and 12 Fe_3O_3 rings in the SGGA+U case. These rings are nonplanar and neighbors share common edges. The three central atoms within the cage seem to stabilize the structures. They are shown with more transparency for both geometries in the right column of Fig. 5. Our T_h symmetry clusters can also be considered as cages with one iron (Fe1) in the middle. This cage consists of 12 Fe_2O_2 and 20 Fe_3O_3 rings if we neglect Fe-Fe bonds within the rings. The central iron is strongly bound to the cage in the SGGA-relaxed structures (12 Fe1-Fe2 bonds), whereas it is only weakly bound ($r_{\text{Fe1-Fe2}} \approx 3.3$ Å) in the SGGA+U cases. It has to be noted that Jones *et al.*[39] report a stable cage structure for $Fe_{12}O_{12}$, which has the same building blocks of Fe_2O_2 and Fe_3O_3 rings as our clusters. The results of Ding *et al.*,[23] however, suggest that cages built from larger rings are energetically not favorable, even to such an extent that their $Fe_{20}O_{30}$ cage structure is found to be unstable and can dissociate into smaller clusters. Furthermore, tendency of forming cagelike iron-oxide clusters has been reported very recently by López *et al.*[24] in the nanometer-size range.

The results for bond lengths, ionic charges, magnetic moments and relative total energies are summarized in Table II for all clusters shown in Fig. 5. Here, in the top panel the number of bonds for each type is explicitly shown in parenthesis. We can see that for the ferromagnetic and ferrimagnetic T_h symmetry clusters the bond lengths and ionic charges do not differ much. It is interesting to find that the number of Fe-Fe bonds is reduced from 54 at SGGA to 18 using SGGA+U according to our bond definition with a cutoff distance of 2.9 Å. In reality the Fe1-Fe2 and Fe2-Fe2 distances increase to about 3.3 Å in both magnetic structures, thus, we do not consider them as direct iron-iron bonds. Having less bonds, the mean of the iron-iron bond lengths decreases at the SGGA+U level of relaxation, while without the exclusion of the above mentioned "bonds" the average distance would increase. The reduction in the number of Fe-Fe bonds is also observed for the C_1 symmetry structure (from 38 to 16), however, here, the mean of the bond lengths increases by 7% using SGGA+U. Concerning the Fe-O bonds we find an increase in their lengths for all considered cluster symmetries and for the C_1 symmetry cluster even the number of such type of bonds is slightly increased (from 92 to 96) when switching to SGGA+U. Altogether, similarly to the $Fe_{13}O_8$ cluster, we see that the SGGA+U description results in longer bonds and increased ionic charges compared to SGGA.

From Table II we observe that the average magnitude of the Fe moments do not differ much for the ferromagnetic and ferrimagnetic T_h symmetry cluster. The moments of the central Fe1 are also very close to each other, whereas more difference is seen for surface Fe2 and Fe3 types. Furthermore, the induced O moments have considerable magnitude, 2% to 8% relative to neighboring Fe moments. In the FM state all O moments are FM coupled to Fe moments. This is also true for O2 (which is bound to Fe3 only) in the ferrimagnetic state but for O1 the situation is more complicated. Since one O1 is bound to two Fe2 and one Fe3 types of iron with opposite moment directions it is not obvious which direction the induced moment on O1 should take. Interestingly, although it forms less bonds to Fe3 than to Fe2 its induced moment shows FM coupling to Fe3, whereas AFM coupling to Fe2. This situation is more understandable for the structure obtained within SGGA+U, where the Fe3-O1 bond is shorter than the one of Fe2-O1. It has to be noted that for a smaller oxygen deficient cluster Fe_9O_6 Sun *et al.*[33] report AFM polarization of O moments with respect to Fe. This difference compared to our finding must be due to the different stoichiometry as well as to cluster topology resulting in different hybridization of O $2p$ and Fe $3d$ orbitals. Moreover, in the C_1 symmetry cluster the average magnitude of the iron moments is somewhat larger than in the T_h symmetry and the O moments are FM coupled to Fe moments. Again, enhancement of Fe moments in all considered structures is observed by applying the Hubbard U term.

From the relative total energies we find that the cagelike structures with C_1 symmetry are energetically preferred compared to higher symmetry clusters for both using SGGA and SGGA+U approaches. The reason of this might be that the cagelike geometry of T_h symmetry clusters is less stabilized via the central iron atom, which is only weakly bound to the cage obtained within SGGA+U ($r_{\text{Fe1-Fe2}} \approx 3.3$ Å). This seems to be partly responsible for the observed total energy difference of about 10 eV between low- and high-symmetry structures. Employing SGGA this energy difference is much smaller (2.23 and 4.76 eV for the two magnetic states) and at the same time the central Fe1 is bound stronger to the cage in the T_h symmetry cases. On the other hand, in the C_1 symmetry clusters one O and two Fe atoms within the cage stabilize the structure with additional Fe-Fe and Fe-O bonds. Another reason for enhanced energetic stability might be the total number of Fe-O bonds, which is larger in the systems of C_1 symmetry than those having T_h.

The results also raise the possibility that iron-oxide clusters at specific stoichiometries prefer to minimize their total magnetic moment indicating a ferrimagnetic arrangement of Fe moments. Such behavior has been reported for bulk iron-oxides, equistoichiometric wüstite (FeO) at low-temperature, oxygen-rich magnetite (Fe_3O_4) and hematite (α-Fe_2O_3) (Ref. 36) and for smaller clusters where the number of O atoms has been equal to or greater than the number of Fe atoms,[36,38] thus, defining the applicable stoichiometry range. On the other hand, results of Kortus *et al.*[31] suggest that iron-rich clusters, where compact iron regions are formed within the iron-oxide structure, prefer FM Fe moment arrangement most likely due to direct exchange for topological reason (see also Sec. III A).

In order to determine the nature of magnetic interactions between Fe ions in our energetically preferred C_1 symmetry oxygen-rich $Fe_{25}O_{30}$ clusters we analyze their electronic properties. Total DOS and contributions from Fe d and O p states are shown in Fig. 6 for these clusters obtained within

TABLE II. Physical properties of the relaxed $Fe_{25}O_{30}$ clusters in two symmetries, the T_h restricted one in ferromagnetic and ferrimagnetic configurations and the unrestricted one (C_1), obtained by using the SGGA ($U^\star=0$) and SGGA+U ($U^\star=5$ eV) approaches. For the C_1 symmetry cluster we found energetically preferred ferromagnetic and ferrimagnetic configurations using SGGA and SGGA+U, respectively. Exact and average bond lengths, ionic charges, atomic, average, and total magnetic moments and total energies relative to the lowest energy structure found for using the corresponding method are shown. Numbers in parentheses refer to the number of bonds of the corresponding type in the bond lengths panel and to the number of that particular atom (see text for details) in the other two panels. Reported values in this table belong to structures shown in Fig. 5.

$Fe_{25}O_{30}$	Symm-T_h-Ferromagnetic				Symm-T_h-Ferrimagnetic				Symmetry C_1	
					Bond lengths (Å)					
Method	SGGA		SGGA+U		SGGA		SGGA+U		SGGA	SGGA+U
$r_{Fe1\text{-}Fe2}$	2.881	(12)			2.855	(12)				
$r_{Fe2\text{-}Fe2}$	2.885	(24)			2.858	(24)				
$r_{Fe2\text{-}Fe3}$	2.735	(12)	2.785		2.725	(12)	2.770			
$r_{Fe3\text{-}Fe3}$	2.280	(6)	2.401		2.337	(6)	2.396			
$\langle r_{Fe\text{-}Fe}\rangle$	2.784	(54)	2.657	(18)	2.770	(54)	2.645	(18)	2.607(38)	2.791(16)
$r_{Fe2\text{-}O1}$	1.878	(48)	1.970		1.868	(48)	1.958			
$r_{Fe3\text{-}O1}$	1.862	(24)	1.892		1.870	(24)	1.895			
$r_{Fe3\text{-}O2}$	1.803	(12)	1.829		1.808	(12)	1.829			
$\langle r_{Fe\text{-}O}\rangle$	1.863	(84)	1.928		1.860	(84)	1.922		1.909(92)	1.989(96)
					Ionic charges [$\lvert e\rvert$]					
Method	SGGA		SGGA+U		SGGA		SGGA+U		SGGA	SGGA+U
q_{Fe1}	+0.158	(1)	+0.330		+0.099	(1)	+0.366			
q_{Fe2}	+1.101	(12)	+1.298		+1.094	(12)	+1.295			
q_{Fe3}	+1.186	(12)	+1.354		+1.205	(12)	+1.341			
$\langle q_{Fe}\rangle$	+1.104	(25)	+1.286		+1.107	(25)	+1.280		+1.145	+1.399
q_{O1}	−0.909	(24)	−1.072		−0.913	(24)	−1.065			
q_{O2}	−0.962	(6)	−1.072		−0.961	(6)	−1.074			
$\langle q_O\rangle$	−0.920	(30)	−1.072		−0.923	(30)	−1.067		−0.954	−1.166
					Magnetic moments [μ_B]					
Method	SGGA		SGGA+U		SGGA		SGGA+U		SGGA	SGGA+U
μ_{Fe1}	3.136	(1)	3.867		3.161	(1)	3.857			
μ_{Fe2}	2.274	(12)	3.665		2.070	(12)	3.604			
μ_{Fe3}	3.008	(12)	3.940		−3.190	(12)	−3.900			
$\langle\lvert\mu_{Fe}\rvert\rangle$	2.661	(25)	3.805		2.651	(25)	3.756		2.817	3.861
μ_{O1}	0.141	(24)	0.129		−0.069	(24)	−0.103			
μ_{O2}	0.152	(6)	0.303		−0.244	(6)	−0.300			
$\langle\lvert\mu_O\rvert\rangle$	0.143	(30)	0.164		0.104	(30)	0.142		0.154	0.189
Total moment	70.8		100.0		−13.4		−4.0		75.1	2.1
Rel. total energy (eV)	4.76		11.30		2.23		10.14		0.00	0.00

SGGA and SGGA+U. A very small HOMO-LUMO gap of 0.03 eV is found for the SGGA case, thus, this cluster is close to half-metallic. The ferrimagnetic C_1 structure is insulating and has a HOMO-LUMO gap of 0.63 eV, the largest among all discussed structures in this stoichiometry. For SGGA we see that minority spin electron DOS comes mostly from *d* states of irons above −2 eV with respect to the Fermi level, while from *p* states of oxygens below that level. For majority spin electrons the *d* character dominates over the whole plotted energy range. Hybridization between Fe *d* and O *p* states is obviously seen throughout. For SGGA+U the *p* states of oxygens are less pronounced above the Fermi level compared to Fe *d* states, while they have at least equal importance below that for both spin channels. In order to decide whether double exchange can take place in the clusters we analyze the Fe *d* shell electron occupancies. By categorizing these into intervals we can count the number of Fe ions in the system having *d* shell electron occupancy within a given range. Following this we can plot a histogram (bottom part of Fig. 8), where we see that the *d* shell electron occupancies are close to that of the neutral iron atom (6) and the maximum difference in the *d* shell between any two iron ions is 0.4 electrons both for SGGA and SGGA+U. This excludes the possibility of double exchange taking place since it requires a valence mismatch of one electron between two nearest neighbor magnetic ions mediated by oxygen. If double exchange can be excluded then we are able to construct a Heisenberg-type Hamiltonian,

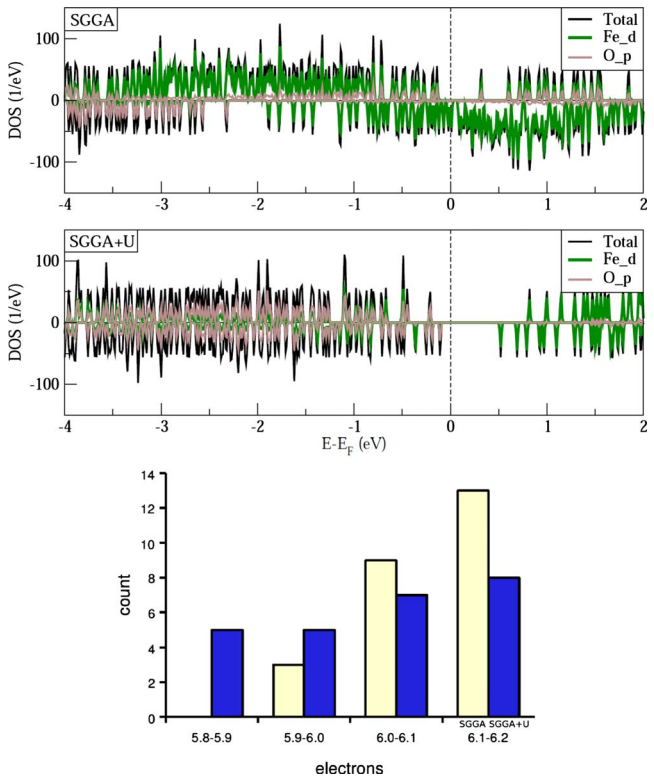

FIG. 6. (Color online) Total electron DOS of the energetically preferred C_1 symmetry clusters of $Fe_{25}O_{30}$ stoichiometry obtained within SGGA (ferromagnetic, top part) and SGGA+U (ferrimagnetic, middle part). Contributions from Fe *d*-type and O *p*-type states are highlighted in green (medium) and gray (light) colors, respectively. Corresponding geometries are shown in the rightmost column of Fig. 5. Histogram of the Fe *d* shell electron occupancies is shown in the bottom part for the mentioned clusters obtained within SGGA (light yellow) and SGGA+U (dark blue).

$$H = \sum_{i,j(\mathrm{Fe}i\text{-}\mathrm{Fe}j)} -J^D_{ij}\underline{S}_i\underline{S}_j + \sum_{i,j(\mathrm{Fe}i\text{-O-}\mathrm{Fe}j)} -J^S_{ij}\underline{S}_i\underline{S}_j, \qquad (2)$$

consisting of spin-spin interactions of directly bound irons (direct exchange term) and nearest-neighbors mediated by oxygen (superexchange term). Thus, we propose a competition between the direct exchange and the superexchange terms in determining the leading order of magnetic interaction. If we assume as first approximation that the exchange parameters are constant each ($J^D > J^S$)[55] and do not depend on *i* and *j* then the importance of the relation of the number of Fe-Fe to the number of Fe-O-Fe bonds becomes clear. For iron-rich clusters the number of Fe-Fe bonds is larger than the Fe-O-Fe bonds, thus the direct exchange term dominates, whereas in the case of oxygen-rich compositions the superexchange term gains more relevance. Since J^D is greater than J^S, and the number of Fe-Fe bonds is not much smaller than the Fe-O-Fe bonds in the cluster obtained within SGGA, the direct exchange term dominates, which can also be seen at the very small HOMO-LUMO gap resulting in close to half-metallicity. On the other hand the number of Fe-Fe bonds is much smaller than the number of Fe-O bonds for the cluster obtained within SGGA+U and the dominant magnetic interaction between iron ions is superexchange as it is also suggested by the large HOMO-LUMO gap. Not surprisingly, the number of Fe-O-Fe bonds is maximal in the latter case among all considered systems. In reality the exchange parameters cannot be treated as constants and the interpretation is more difficult, particularly due to the strong dependence of J^S_{ij} on the Fe*i*-O-Fe*j* bond angle, but the underlying physics is highlighted in our simple model. Furthermore, in contrast to the C_1 symmetry structures, it is noticed that Fe pairs of mixed valency are found in all of our high symmetry clusters, where the central iron ion (Fe1) has always almost one electron less than neighboring (Fe2) ones. Concomitantly we obtain HOMO-LUMO gaps of less than 0.15 eV in these clusters.

C. $Fe_{33}O_{32}$

Finally, we choose an iron-oxide cluster with a very close to 1:1 stoichiometry. Starting from numerous initial geometries the energetically preferred structures are summarized in Fig. 7 (top panel for SGGA, bottom panel for SGGA+U) for each considered symmetry and magnetic state. Here, labels of the individual structures refer to their relative total energies (in eV) compared to the lowest lying one, which is denoted by zero. Note that comparison of energies is only meaningful within particular panels using the same approximation.

By building initial cluster geometries we did the following: O_h symmetry clusters have been designed by taking the O_h symmetry $Fe_{13}O_8$ structure (Sec. III A) as core and then added 20 Fe and 24 O atoms to it in different ways retaining symmetry. In this way we end up with five nonequivalent iron and two nonequivalent oxygen atoms within the cluster. The energetically preferred ferrimagnetic state is chosen from a set of calculations taking fifteen possible collinear iron moment arrangements into account. For symmetry-unrestricted relaxations resulting in clusters of C_1 symmetry we consider one ferrimagnetic state only and do not calculate all possible magnetic states. Moreover, a third type of cluster with a perfect rocksalt structure has been designed, which consists of a cube ($4\times4\times4$) of alternating Fe and O atoms such as a block cut out from the bulk FeO crystal and an additional iron atom in order to comply with the $Fe_{33}O_{32}$ composition. For this cluster type we compare two different ferrimagnetic states and the energetically preferred one is reported. Using SGGA this structure becomes much distorted from a perfect rocksalt cluster after relaxation. Such distortion due to AFM Co atomic moment arrangement has been previously reported for the smaller Co_4O_4 cluster,[37] however, in our case this structure is energetically preferred compared to a FM rocksalt cluster. Furthermore, we observe that relaxations using SGGA+U result in structures closer to a perfect rocksalt geometry than in the case of SGGA. This is due to the enhanced ionic charges using the SGGA+U approach (Table III) compared to SGGA as we have seen in previous systems. We find the same tendency for this stoichiometry in all structures.

The results for average bond lengths, ionic charges, mean and total magnetic moments as well as relative total energies

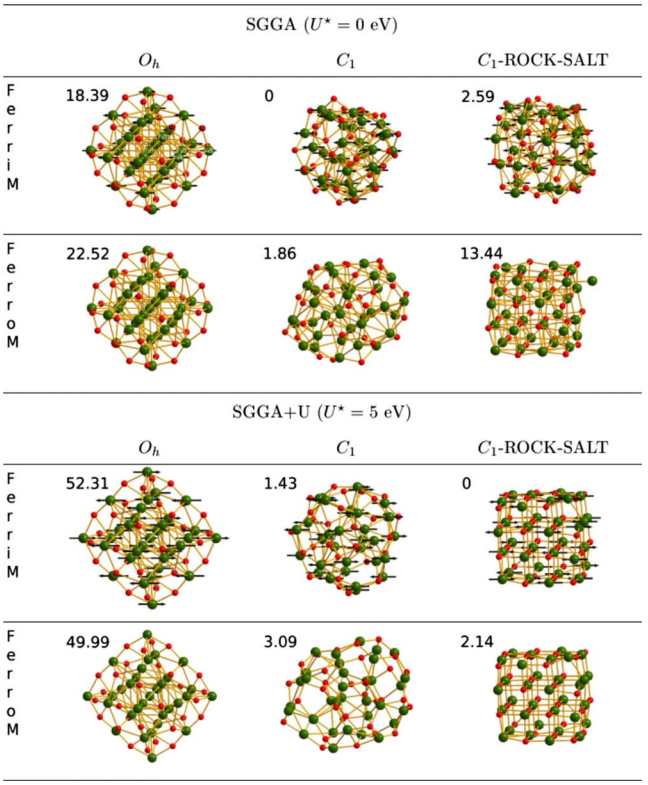

FIG. 7. (Color online) Relaxed geometries of the $Fe_{33}O_{32}$ cluster obtained in the O_h-restricted (left) and symmetry-unrestricted (middle and right) optimizations at the SGGA ($U^\star$=0 eV) (top panel) and SGGA+U ($U^\star$=5 eV) (bottom panel) levels of approximation for ferrimagnetic and ferromagnetic configurations. Each structure is labeled (at the top left part) by its total energy (in eV) relative to the calculated lowest value, which is denoted by zero. Note that comparison of energies is only meaningful within particular panels using the same approximation. Middle column shows clusters with C_1 symmetry while the right column shows rocksalt type structures. Calculated Fe atomic magnetic moment vectors are shown for the ferrimagnetic configurations only. Fe and O atoms are denoted by green (dark) and red (light) colors, respectively. Bonding and magnetic properties of these structures are reported in Table III.

are summarized in Table III for all clusters shown in Fig. 7. The total number of bonds of each type is explicitly shown in parenthesis. Here, similar trends can be observed as in the $Fe_{25}O_{30}$ clusters (Sec. III B), namely, the number of Fe-Fe bonds decreases and their average length increases by switching from SGGA to SGGA+U type of relaxations. In this case the reduced number of bonds is more pronounced in the clusters showing low symmetry (C_1 and rocksalt structures) and the mean of their bond lengths is also larger than for the O_h symmetry structures. For Fe-O bonds it is generally true that their number and average length increase with the exception of the FM rocksalt cluster where the number of Fe-O bonds slightly drops. Furthermore, the number and average length of Fe-O bonds are larger for the rocksalt structures, for both SGGA and SGGA+U, compared to the other two types.

From Table III it can be seen that the average magnitude of the Fe moments in the ferrimagnetic and ferromagnetic states do not differ much in the clusters with low symmetry. However, this difference is considerable in the high symmetry O_h clusters. Comparing the mean of the Fe moment magnitudes between different symmetries we find that they are larger in the clusters having lower symmetry (C_1) compared to the high symmetry (O_h) ones only for SGGA and not when using SGGA+U. Again, enhancement of Fe moments in all considered structures is observed applying the Hubbard U term. It is also interesting to see that the average magnitudes of induced O moments are systematically less in the ferrimagnetic states compared to the FM ones. This might be due to the O atoms experiencing competing effects of spin polarization originating from neighboring oppositely aligned Fe magnetic moments as has been indicated for O1 types of oxygen in the T_h symmetry $Fe_{25}O_{30}$ cluster and discussed in Sec. III B. On the other hand, for the ferromagnetic clusters all O moments are FM coupled to Fe moments. We can also observe that the mean of the O moment magnitudes increases only in the O_h symmetry structures by switching from SGGA to SGGA+U, whereas in the low-symmetry structures they drop upon this switching. On average, we find the largest induced O moments in the FM O_h symmetry clusters both in absolute value and relative to the average magnitude of Fe moments (close to 10% for both SGGA and SGGA+U). Comparing total energies, however, shows that such a combination of geometry and magnetism is far from being favored.

Among the studied systems we find the ferrimagnetic C_1 symmetry cluster energetically favored using SGGA, while the ferrimagnetic rocksalt structure in the SGGA+U case. This structural variety is due to the different valency of iron ions depending on the U parameter. On the other hand these structures have also similarities. Both clusters have the majority of their atoms on their surface. Moreover, as discussed above, they both have low externally observable total magnetic moments, less than $4\mu_B$. In order to determine the dominant magnetic interaction between Fe ions in these clusters we study their electronic properties in more detail. Total DOS and contributions from Fe d and O p states are shown in Fig. 8. For SGGA we see that electron DOS comes mostly from d states of irons above −3.5 eV with respect to the Fermi level. Hybridization between Fe d and O p states is seen through the whole plotted energy range. For SGGA +U the p states of oxygens are less pronounced above the Fermi level compared to Fe d states, whereas they have mostly equal importance below that. By plotting a histogram of the d shell electron occupancy considering each Fe ion (bottom part of Fig. 8), we see that it is close to the occupancy of the neutral iron atom (6) and the difference in the d shell between any two iron ions is less than 0.4 electrons both for SGGA and SGGA+U. Therefore, as we have found in the C_1 symmetry $Fe_{25}O_{30}$ clusters, double exchange can be excluded from possible magnetic interactions. Thus, following Eq. (2), while the number of Fe-Fe bonds is significant for the structure obtained within SGGA, it is much smaller than the number of Fe-O-Fe bonds in the cluster obtained by using SGGA+U. This suggests that direct exchange plays a more important role in the former cluster, which is also indicated by the small HOMO-LUMO gap of 0.10 eV. On the other hand, superexchange is more important for topological

TABLE III. Physical properties of the relaxed $Fe_{33}O_{32}$ clusters in the O_h and unrestricted (C_1) symmetries as well as in rocksaltlike structure, obtained by using the SGGA ($U^\star=0$) and SGGA+U ($U^\star=5$ eV) approaches. Both ferromagnetic and ferrimagnetic configurations are reported for all considered geometry types. Average bond lengths, average ionic charges, average atomic, and total magnetic moments and total energies relative to the lowest energy structure found for using the corresponding method are shown. Numbers in parentheses refer to number of bonds of the corresponding type in the cluster. Reported values in this table belong to structures shown in Fig. 7.

$Fe_{33}O_{32}$	SGGA						SGGA+U					
Structure	Ave. bond lengths (Å)		Ave. ionic charge [$\|e\|$]	Magnetic moments [μ_B]		Rel. total	Ave. bond lengths (Å)		Ave. ionic charge [$\|e\|$]	Magnetic moments [μ_B]		Rel. total
	$\langle r_{Fe\text{-}Fe}\rangle$	$\langle r_{Fe\text{-}O}\rangle$	$\langle q_{Fe}\rangle$	$\langle\|\mu_{Fe}\|\rangle$	Total	energy	$\langle r_{Fe\text{-}Fe}\rangle$	$\langle r_{Fe\text{-}O}\rangle$	$\langle q_{Fe}\rangle$	$\langle\|\mu_{Fe}\|\rangle$	Total	energy
Magnetic Config.			$\langle q_O\rangle$	$\langle\|\mu_O\|\rangle$		(eV)			$\langle q_O\rangle$	$\langle\|\mu_O\|\rangle$		(eV)
O_h	2.524	1.813	+0.788	2.500	90.9	22.52	2.621	1.991	+0.974	3.745	134.7	49.99
FerroM.	(92)	(56)	−0.813	0.263			(74)	(80)	−1.004	0.348		
O_h	2.533	1.802	+0.790	2.259	7.3	18.39	2.598	2.016	+0.962	3.652	21.0	52.31
FerriM.	(104)	(56)	−0.815	0.050			(74)	(80)	−0.992	0.112		
C_1	2.613	1.940	+0.971	2.824	98.6	1.86	2.781	2.020	+1.184	3.689	126.6	3.09
FerroM.	(71)	(106)	−1.002	0.164			(28)	(111)	−1.221	0.153		
C_1	2.615	1.925	+0.976	2.834	0.3	0.00	2.765	1.991	+1.175	3.641	2.1	1.43
FerriM.	(67)	(103)	−1.007	0.070			(27)	(109)	−1.212	0.058		
Rocksalt	2.652	2.050	+1.065	2.964	104.6	13.44	2.722	2.110	+1.213	3.745	128.1	2.14
FerroM.	(58)	(143)	−1.099	0.214			(12)	(142)	−1.251	0.140		
Rocksalt	2.616	1.966	+0.989	2.961	−5.7	2.59	2.748	2.110	+1.207	3.701	−3.7	0.00
FerriM.	(65)	(109)	−1.020	0.081			(14)	(144)	−1.245	0.055		

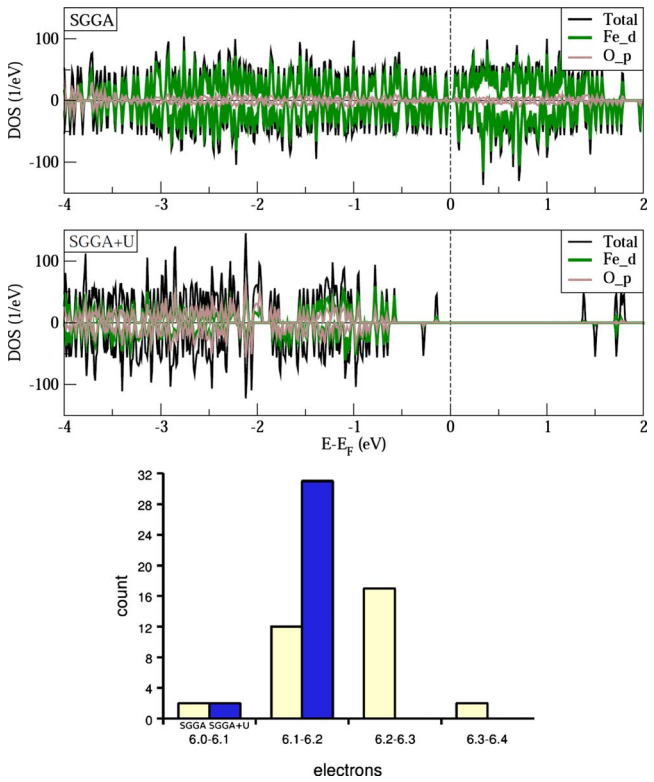

FIG. 8. (Color online) Total electron DOS of the energetically preferred C_1 symmetry clusters of $Fe_{33}O_{32}$ stoichiometry obtained within SGGA (C_1, ferrimagnetic, top part) and SGGA+U (C_1 rocksalt, ferrimagnetic, middle part). Contributions from Fe *d*-type and O *p*-type states are highlighted in green (medium) and gray (light) colors, respectively. Corresponding geometries are labeled by "0" in Fig. 7. Histogram of the Fe *d* shell electron occupancies is shown in the bottom part for the mentioned clusters obtained within SGGA (light yellow) and SGGA+U (dark blue).

reasons for the rocksalt cluster, which has a large gap of 1.53 eV. Note that for this cluster the number of Fe-O-Fe bonds is maximal among all considered systems.

Summarized, we find the ferrimagnetic C_1 symmetry cluster and the ferrimagnetic rocksalt cluster energetically favored, using SGGA and SGGA+U ($U^{\star}=5$ eV), respectively. They are both labeled by "0" in Fig. 7 (SGGA: top, SGGA+U: bottom panel). Based on our results we conclude that ferrimagnetic clusters are energetically preferred compared to their FM counterparts having very similar geometry with the only exception of the O_h symmetry clusters in the SGGA+U case. However, total energies of these high symmetry clusters are very far from the lowest observed one, thus, they can definitely be excluded from possible ground states. For the most likely ground-state geometries of low symmetry the energy differences between ferrimagnetic and ferromagnetic states are found to be at least 1.66 eV in favor of ferrimagnetism. This finding for intermediate cluster size fits well between smaller clusters and bulk iron-oxides, i.e., ferrimagnetism has been observed in smaller clusters[38] and in bulk Fe_3O_4,[9] while for stoichiometric bulk FeO a perfect AFM ordering of the iron moments has been reported.[4]

IV. CONCLUSIONS

In the present work we performed spin-polarized DFT simulations within GGA and GGA+U levels of approximation on nanometer-sized iron-oxide atomic clusters in different stoichiometries. Due to the large size of the clusters we have focused on the energetic comparison between isostoichiometric structures having different symmetries and also between their selected collinear ferromagnetic and ferrimagnetic states. We found that low-symmetry geometries are energetically preferred compared to high symmetry ones for the whole studied stoichiometry range.

We have presented results for the smaller well-studied iron-rich $Fe_{13}O_8$ cluster where we obtained energetically more favorable low-symmetry structures than previously reported. Studying the effect of the Hubbard U parameter on the electronic and magnetic properties we found that the HOMO-LUMO gap can change nonmonotonously, while the average iron moments show a linear dependence on U in most of the studied range.

Regarding cluster structures in the nanometer-size regime we found the following: For the oxygen-rich $Fe_{25}O_{30}$ stoichiometry we obtained cagelike geometries with a few ions within the cage, which seem to stabilize the structure. For a close to stoichiometric $Fe_{33}O_{32}$ cluster we found a less ordered C_1 symmetry structure favored when using GGA, while a more ordered rocksalt type cluster, reminiscent of the bulk FeO phase, for GGA+U. This result shows how the structures are sensitive to the method used for describing exchange correlation in TMO clusters. We point out that significant structural changes occur by switching from GGA to GGA+U during geometrical relaxation. An indication of the structural change is the increase in the bond lengths observed at the GGA+U level of description, which is due to the enhanced anion-anion and cation-cation types of electrostatic repulsion resulting from increased ionic charges. We also suggest that experimental measurement of valence states of individual ions in small clusters could help in the better understanding of their structure. Based on our results, we propose that at close to 1:1 stoichiometry a rocksalt type cluster with alternating Fe and O ions in the lattice points of a simple cubic lattice starts to form at as small as close to nanometer-size. This structure seems to maximize the number of Fe-O and Fe-O-Fe bonds and concomitantly minimize the number of Fe-Fe bonds. For this size and constitution we did not find cagelike geometries, which were found to be more stable at smaller cluster sizes.

By performing total energy comparison we propose that the studied clusters in the nanometer-size regime prefer ferrimagnetic states compared to ferromagnetic ones. The results suggest that this behavior applies only to iron-oxide clusters of either having a close to stoichiometric one to one composition or in the presence of excess oxygen within the cluster. Moreover, based on data of Fe *d* shell electron occupancies, we exclude double exchange from possible magnetic interactions between iron ions, and our results point to a competition between direct exchange and superexchange, where the dominant interaction is determined by the cluster topology with the number of Fe-Fe and Fe-O-Fe bonds

playing an important role. In addition, information about the nature of the dominant magnetic interaction can be drawn from the electronic structure, at first instance from the magnitude of the HOMO-LUMO gap of the cluster.

Altogether, our results demonstrate the importance of going beyond GGA, in particular, physical properties obtained within GGA+U description are found to be remarkably different from those using GGA, such as bond lengths depend substantially on ionic charges, concomitantly resulting in a switching of dominant magnetic interactions between iron ions. In order to confirm our theoretical predictions, cluster experiments in this size regime are desirable.

ACKNOWLEDGMENTS

The Marie Curie Transfer of Knowledge program of the European Commission (NANOTAIL, Grant No. MTKD-CT-2006-042459) is acknowledged for providing financial support. Furthermore, K.P. acknowledges support from the Magyary Foundation, EEA and Norway Grants for finalizing this study and also thanks H. P. Pinto for useful discussions.

*Present address: Budapest University of Technology and Economics, Department of Theoretical Physics, Budafoki út 8., H-1111 Budapest, Hungary; palotas@phy.bme.hu

[1] E. M. L. Plumer, J. van Ek, and D. Weller, *The Physics of Ultra-High Density Magnetic Recording, Springer Series in Surface Science* (Springer, Berlin, Germany, 2001), Vol. 41.
[2] N. Weiss, T. Cren, M. Epple, S. Rusponi, G. Baudot, S. Rohart, A. Tejeda, V. Repain, S. Rousset, P. Ohresser, F. Scheurer, P. Bencok, and H. Brune, Phys. Rev. Lett. **95**, 157204 (2005).
[3] J.-H. Park, G. von Maltzahn, L. Zhang, M. P. Schwartz, E. Ruoslahti, S. N. Bhatia, and M. J. Sailor, Adv. Mater. **20**, 1630 (2008).
[4] M. Alfredsson, G. D. Price, C. R. A. Catlow, S. C. Parker, R. Orlando, and J. P. Brodholt, Phys. Rev. B **70**, 165111 (2004).
[5] J. Cheon, N.-J. Kang, S.-M. Lee, J.-H. Lee, J.-H. Yoon, and S. J. Oh, J. Am. Chem. Soc. **126**, 1950 (2004).
[6] L. Berger, Y. Labaye, M. Tamine, and J. M. D. Coey, Phys. Rev. B **77**, 104431 (2008).
[7] J. Mazo-Zuluaga, J. Restrepo, and J. Mejia-López, J. Appl. Phys. **103**, 113906 (2008).
[8] K. Palotás, B. Lazarovits, L. Szunyogh, and P. Weinberger, Phys. Rev. B **67**, 174404 (2003).
[9] L. Wang, T. Maxisch, and G. Ceder, Phys. Rev. B **73**, 195107 (2006).
[10] V. I. Anisimov, I. S. Elfimov, N. Hamada, and K. Terakura, Phys. Rev. B **54**, 4387 (1996).
[11] I. I. Mazin and V. I. Anisimov, Phys. Rev. B **55**, 12822 (1997).
[12] V. N. Antonov, B. N. Harmon, V. P. Antropov, A. Y. Perlov, and A. N. Yaresko, Phys. Rev. B **64**, 134410 (2001).
[13] D. J. Huang, C. F. Chang, H.-T. Jeng, G. Y. Guo, H.-J. Lin, W. B. Wu, H. C. Ku, A. Fujimori, Y. Takahashi, and C. T. Chen, Phys. Rev. Lett. **93**, 077204 (2004).
[14] I. Leonov, A. N. Yaresko, V. N. Antonov, M. A. Korotin, and V. I. Anisimov, Phys. Rev. Lett. **93**, 146404 (2004).
[15] H.-T. Jeng, G. Y. Guo, and D. J. Huang, Phys. Rev. Lett. **93**, 156403 (2004).
[16] H. P. Pinto and S. D. Elliott, J. Phys.: Condens. Matter **18**, 10427 (2006).
[17] A. Rohrbach, J. Hafner, and G. Kresse, Phys. Rev. B **69**, 075413 (2004).
[18] B. V. Reddy and S. N. Khanna, Phys. Rev. Lett. **93**, 068301 (2004).
[19] N. M. Reilly, J. U. Reveles, G. E. Johnson, S. N. Khanna, and A. W. Castleman, Jr., Chem. Phys. Lett. **435**, 295 (2007).
[20] N. M. Reilly, J. U. Reveles, G. E. Johnson, J. M. del Campo, S. N. Khanna, A. M. Koster, and A. W. Castleman, Jr., J. Phys. Chem. C **111**, 19086 (2007).
[21] N. M. Reilly, J. U. Reveles, G. E. Johnson, S. N. Khanna, and A. W. Castleman, Jr., J. Phys. Chem. A **111**, 4158 (2007).
[22] Z. Szotek, W. M. Temmerman, D. Ködderitzsch, A. Svane, L. Petit, and H. Winter, Phys. Rev. B **74**, 174431 (2006).
[23] X.-L. Ding, W. Xue, Y.-P. Ma, Z.-C. Wang, and S.-G. He, J. Chem. Phys. **130**, 014303 (2009).
[24] S. López, A. H. Romero, J. Mejía-López, J. Mazo-Zuluaga, and J. Restrepo, Phys. Rev. B **80**, 085107 (2009).
[25] L.-S. Wang, H. Wu, and S. R. Desai, Phys. Rev. Lett. **76**, 4853 (1996).
[26] L.-S. Wang, J. W. Fan, and L. Lou, Surf. Rev. Lett. **3**, 695 (1996).
[27] J. B. Griffin and P. B. Armentrout, J. Chem. Phys. **106**, 4448 (1997).
[28] Q. Wang, Q. Sun, M. Sakurai, J. Z. Yu, B. L. Gu, K. Sumiyama, and Y. Kawazoe, Phys. Rev. B **59**, 12672 (1999).
[29] M. Sakurai, K. Sumiyama, Q. Sun, and Y. Kawazoe, J. Phys. Soc. Jpn. **68**, 3497 (1999).
[30] Q. Sun, Q. Wang, K. Parlinski, J. Z. Yu, Y. Hashi, X. G. Gong, and Y. Kawazoe, Phys. Rev. B **61**, 5781 (2000).
[31] J. Kortus and M. R. Pederson, Phys. Rev. B **62**, 5755 (2000).
[32] Q. Sun, B. V. Reddy, M. Marquez, P. Jena, C. Gonzalez, and Q. Wang, J. Phys. Chem. C **111**, 4159 (2007).
[33] Q. Sun, M. Sakurai, Q. Wang, J. Z. Yu, G. H. Wang, K. Sumiyama, and Y. Kawazoe, Phys. Rev. B **62**, 8500 (2000).
[34] D. N. Shin, Y. Matsuda, and E. R. Bernstein, J. Chem. Phys. **120**, 4150 (2004).
[35] D. N. Shin, Y. Matsuda, and E. R. Bernstein, J. Chem. Phys. **120**, 4157 (2004).
[36] H. Shiroishi, T. Oda, I. Hamada, and N. Fujima, Eur. Phys. J. D **24**, 85 (2003).
[37] A. Kirilyuk, K. Demyk, G. von Heiden, G. Meijer, A. I. Poteryaev, and A. I. Lichtenstein, J. Appl. Phys. **93**, 7379 (2003).
[38] N. O. Jones, B. V. Reddy, F. Rasouli, and S. N. Khanna, Phys. Rev. B **72**, 165411 (2005).
[39] N. O. Jones, B. V. Reddy, F. Rasouli, and S. N. Khanna, Phys. Rev. B **73**, 119901(E) (2006).
[40] K. S. Molek, C. Anfuso-Cleary, and M. A. Duncan, J. Phys. Chem. A **112**, 9238 (2008).
[41] S. Yin, W. Xue, X.-L. Ding, W.-G. Wang, S.-G. He, and M.-F. Ge, Int. J. Mass Spectrom. **281**, 72 (2009).
[42] G. Kresse and J. Hafner, Phys. Rev. B **47**, 558 (1993).
[43] G. Kresse and J. Furthmüller, Comput. Mater. Sci. **6**, 15 (1996).

[44] G. Kresse and J. Furthmüller, Phys. Rev. B **54**, 11169 (1996).
[45] J. Hafner, J. Comput. Chem. **29**, 2044 (2008).
[46] S. L. Dudarev, G. A. Botton, S. Y. Savrasov, C. J. Humphreys, and A. P. Sutton, Phys. Rev. B **57**, 1505 (1998).
[47] G. Kresse and D. Joubert, Phys. Rev. B **59**, 1758 (1999).
[48] J. P. Perdew and Y. Wang, Phys. Rev. B **45**, 13244 (1992).
[49] G. Henkelman, A. Arnaldsson, and H. Jónsson, Comput. Mater. Sci. **36**, 354 (2006).
[50] E. Sanville, S. D. Kenny, R. Smith, and G. Henkelman, J. Comput. Chem. **28**, 899 (2007).
[51] W. Tang, E. Sanville, and G. Henkelman, J. Phys.: Condens. Matter **21**, 084204 (2009).
[52] M. Cococcioni and S. de Gironcoli, Phys. Rev. B **71**, 035105 (2005).
[53] H. J. Kulik, M. Cococcioni, D. A. Scherlis, and N. Marzari, Phys. Rev. Lett. **97**, 103001 (2006).
[54] R. L. Johnston, Dalton Trans. 4193 (2003).
[55] W. A. Harrison, Phys. Rev. B **76**, 054417 (2007).